Decoration of Outer Membrane Vesicles with Multiple Antigens by Using an Autotransporter Approach

Maria H. Daleke-Schermerhorn, Tristan Felix, Zora Soprova, Corinne M. ten Hagen-Jongman, Vikström David, Laleh Majlessi, Beskers Joep, Frank Follmann, Karin de Punder, Nicole N. van Der Wel, et al.

AEM
Journals.ASM.org

Decoration of Outer Membrane Vesicles with Multiple Antigens by Using an Autotransporter Approach

Maria H. Daleke-Schermerhorn,[a,b] Tristan Felix,[c,d] Zora Soprova,[a] Corinne M. ten Hagen-Jongman,[a,b] David Vikström,[e,f] Laleh Majlessi,[c,d*] Joep Beskers,[a] Frank Follmann,[g] Karin de Punder,[h*] Nicole N. van der Wel,[h*] Thomas Baumgarten,[e] Thang V. Pham,[i] Sander R. Piersma,[i] Connie R. Jiménez,[i] Peter van Ulsen,[a] Jan-Willem de Gier,[e] Claude Leclerc,[c,d] Wouter S. P. Jong,[a,b] Joen Luirink[a,b]

Section Molecular Microbiology, Department of Molecular Cell Biology, Faculty of Earth and Life Sciences, VU University, Amsterdam, The Netherlands[a]; Abera Bioscience AB, Stockholm, Sweden[b]; Institut Pasteur, Unité de Régulation Immunitaire et Vaccinologie, Paris, France[c]; INSERM, U1041, Paris, France[d]; Center for Biomembrane Research, Department of Biochemistry and Biophysics, Stockholm University, Stockholm, Sweden[e]; Xbrane Bioscience AB, Stockholm, Sweden[f]; Chlamydia Vaccine Research, Department of Infectious Disease Immunology, Statens Serum Institut, Copenhagen, Denmark[g]; The Netherlands Cancer Institute, Antonie van Leeuwenhoek Hospital, Amsterdam, The Netherlands[h]; Department of Medical Oncology, OncoProteomics Laboratory, VU University Medical Center, Amsterdam, The Netherlands[i]

Outer membrane vesicles (OMVs) are spherical nanoparticles that naturally shed from Gram-negative bacteria. They are rich in immunostimulatory proteins and lipopolysaccharide but do not replicate, which increases their safety profile and renders them attractive vaccine vectors. By packaging foreign polypeptides in OMVs, specific immune responses can be raised toward heterologous antigens in the context of an intrinsic adjuvant. Antigens exposed at the vesicle surface have been suggested to elicit protection superior to that from antigens concealed inside OMVs, but hitherto robust methods for targeting heterologous proteins to the OMV surface have been lacking. We have exploited our previously developed hemoglobin protease (Hbp) autotransporter platform for display of heterologous polypeptides at the OMV surface. One, two, or three of the *Mycobacterium tuberculosis* antigens ESAT6, Ag85B, and Rv2660c were targeted to the surface of *Escherichia coli* OMVs upon fusion to Hbp. Furthermore, a hypervesiculating Δ*tolR* Δ*tolA* derivative of attenuated *Salmonella enterica* serovar Typhimurium SL3261 was generated, enabling efficient release and purification of OMVs decorated with multiple heterologous antigens, exemplified by the *M. tuberculosis* antigens and epitopes from *Chlamydia trachomatis* major outer membrane protein (MOMP). Also, we showed that delivery of *Salmonella* OMVs displaying Ag85B to antigen-presenting cells *in vitro* results in processing and presentation of an epitope that is functionally recognized by Ag85B-specific T cell hybridomas. In conclusion, the Hbp platform mediates efficient display of (multiple) heterologous antigens, individually or combined within one molecule, at the surface of OMVs. Detection of antigen-specific immune responses upon vesicle-mediated delivery demonstrated the potential of our system for vaccine development.

Gram-negative bacteria naturally release 20- to 250-nm spherical, bilayered structures known as outer membrane vesicles (OMVs) from their surfaces (1). These OMVs are formed by bulging and pinching off a portion of the outer membrane (OM) and consequently contain lipopolysaccharide (LPS), phospholipids, and the major outer membrane proteins (OMPs) typically found in the Gram-negative OM (2, 3). However, the protein composition of OMVs differs slightly from that of the OM as some proteins are enriched in the vesicles while others are excluded (2, 4–6). OMVs also contain soluble periplasmic components, which become entrapped in the lumen during vesiculation, but very little inner membrane (IM) and cytoplasmic material (2, 4). OMVs have been detected under a variety of culture conditions and natural environments (1) and in infected blood and host tissue (7, 8), and they are believed to play important roles in bacterial growth, survival (9, 10), and virulence (8, 11, 12).

OMVs are loaded with LPS and immunogenic proteins, which allow them to stimulate the innate immune system and simultaneously trigger antigen-specific humoral and $CD4^+$ T cell responses (13). Furthermore, OMVs can be produced in large amounts using hypervesiculating strains that carry genetic mutations affecting certain cell envelope proteins, most notably in the *tol-pal* system (14), and they are easily separated from their parent bacteria by filtration and differential centrifugation methods (15). These properties make OMVs attractive as vaccines. Importantly, mice immunized with OMVs are protected against challenge with virulent bacteria (13, 16, 17), and OMV vaccines against *Neisseria meningitidis* serogroup B (MenB) have been shown to offer protection and are routinely and safely administered to humans in vaccine programs (18).

Several recent studies have shown that heterologous proteins can be targeted to OMVs upon production in the OM or periplasm (19, 20) or as translational fusions to vesicle-associated proteins (21, 22), opening up the interesting possibility of equipping OMVs with an engineered antigen repertoire. An increasing body of evidence suggests that extracellular antigens evoke im-

Received 12 June 2014 **Accepted** 10 July 2014
Published ahead of print 18 July 2014
Editor: H. L. Drake
Address correspondence to Maria H. Daleke-Schermerhorn, maria.daleke@aberabio.com, or Joen Luirink, s.luirink@vu.nl.
* Present address: Laleh Majlessi, UP Pathogénomique Mycobactérienne Intégrée, Institut Pasteur, Paris, France; Karin de Punder, Institute for Medical Psychology, Charité Universitätsmedizin, Berlin, Germany; Nicole N. van der Wel, Department of Cell Biology and Histology, Academic Medical Center, University of Amsterdam, Amsterdam, The Netherlands.

doi:10.1128/AEM.01941-14

mune responses superior to those of intracellular antigens (23–25). Recently, antibody responses to a heterologous antigen packaged into the lumen of *Salmonella* OMVs were observed to be lower than those to endogenous vesicle OMPs and LPS (20), suggesting that surface-exposed antigens may elicit superior immune responses also in vesicles.

We recently engineered the *Escherichia coli* autotransporter (AT) hemoglobin protease (Hbp) into a platform for high-density surface display of heterologous proteins in Gram-negative bacteria (26). The AT pathway is one of the mechanisms that have evolved in Gram-negative bacteria to transfer proteins across their complicated cell envelopes, and it is used for secretion of large virulence factors (27). ATs comprise three domains: an N-terminal signal peptide that mediates translocation across the IM, a central passenger domain that forms the functional part of the protein, and a C-terminal β-domain that inserts into the OM and facilitates translocation of the passenger to the bacterial surface or medium (27). Because ATs combine a relatively simple secretion mechanism with a flexible transport capacity, they have attracted attention as carriers for transport of heterologous proteins to the extracellular milieu (28, 29). For this purpose, heterologous sequences have most often been fused directly to the C-terminal β-domain or to the N terminus of the passenger domain (27, 30, 31). We took a slightly different approach, capitalizing on the crystal structure of the Hbp passenger. The mature Hbp passenger folds into an ~100-Å β-helical stem structure that functions as a stable scaffold for five protruding side domains (d1 to d5) (32). We showed that these side domains are dispensable for translocation and that they can be replaced by heterologous polypeptides (26). In combination with a mutation in the β-domain that prevents release of the passenger domain (Fig. 1A) (33–35), optimal exposure of heterologous proteins can be achieved at some distance from the cell surface (26).

Here, we show, as exemplified by well-known antigens from *Mycobacterium tuberculosis*, that the Hbp platform can be used to achieve high-density exposure of multiple full-length heterologous antigens at the surface of both *E. coli* and *Salmonella* OMVs, with minimal perturbation of the natural OMV protein composition. Importantly, we show that *M. tuberculosis* antigens displayed at the surface of *Salmonella* OMVs are processed and presented by antigen-presenting cells in a manner resembling the situation during natural mycobacterial infection. Furthermore, two B and T cell epitope-containing internal fragments of the *Chlamydia trachomatis* major outer membrane protein (MOMP) were efficiently displayed at the surface of *Salmonella* OMVs. This demonstrated how the Hbp platform can be used for expression of antigenically important polypeptides that are difficult to produce recombinantly in native full-length form. Collectively, the data demonstrate the potential of our approach for OMV vaccine development.

MATERIALS AND METHODS

Bacterial strains and growth conditions. *E. coli* strain JC8031 (Δ*tolRA*) (36), *Salmonella enterica* serovar Typhimurium SL3261 (37), and the isogenic SL3261 Δ*tolRA* mutant strain constructed in this study were grown at 37°C in LB medium containing 0.2% glucose. When appropriate, kanamycin was used at a concentration of 50 μg/ml (*E. coli*) or 25 μg/ml (*S.* Typhimurium), and chloramphenicol was used at a concentration of 30 μg/ml.

Plasmids. Open reading frames (ORFs) encoding Hbp (derivatives) were expressed under the control of a *lacUV5* promoter from pEH3 (38) plasmids. All plasmids were based on pEH3-HbpD(ΔBamHI) (34), in which the sequence encoding the passenger–β-domain junction has been altered to prevent autocatalytic intradomain cleavage. For expression of Hbp lacking side domain d1, we made use of a previously described derivative of pEH3-HbpD(ΔBamHI), pHbp(Δd1) (26), in which the sequence encoding d1 has been substituted for Gly/Ser-encoding linker sequences containing SacI and BamHI restriction sites. HbpD-ESAT6, a chimera in which d1 of Hbp was replaced by the *M. tuberculosis* antigen ESAT6, was expressed from plasmid pHbpD(Δd1)-ESAT6 (26). In this plasmid, a SacI/BamHI-flanked *E. coli* codon-optimized fragment corresponding to *M. tuberculosis esxA* was inserted into the SacI and BamHI sites of pHbp(Δd1). Two additional plasmids, pHbpD-Ag85B$_{C+N}$-ESAT6 and pHbpD-Ag85B$_{C+N}$-ESAT6-Rv2660c (W. S. P. Jong, M. H. Daleke-Schermerhorn, and J. Luirink, unpublished data), were used for expression of HbpD-Ag85B$_{C+N}$-ESAT6 and HbpD-Ag85B$_{C+N}$-ESAT6-Rv2660c. In the *hbp* ORFs of these plasmids, the sequences encoding d1, d2, d4, and d5 had been substituted for Gly/Ser-encoding linker sequences containing SacI and BamHI restriction sites. Subsequently, SacI/BamHI-flanked PCR fragments of *M. tuberculosis* H37Rv *fbpA* encoding an N-terminal (Ag85B$_N$; amino acids [aa] 1 to 126) and a C-terminal (Ag85B$_C$; aa 118 to 285) portion of Ag85B were inserted into the positions corresponding to d2 and d1, respectively, while the above-mentioned *esxA* fragment replaced the d4-encoding sequence. In pHbpD-Ag85B$_{C+N}$-ESAT6-Rv2660c, a PCR fragment of *M. tuberculosis* H37Rv *rv2660c* additionally replaced the sequence coding for d5. For expression of HbpD-MOMPIV-MOMPII, a chimera in which domains d1 and d2 of the Hbp passenger were replaced by Gly/Ser-flanked sequences corresponding to residues 266 to 350 (MOMPIV) and 155 to 190 (MOMPII) of *C. trachomatis* D/UW-3/CX MOMP, plasmid pHbpD-MOMPIV-MOMPII was used (Jong et al., unpublished). In this plasmid, *E. coli* codon-optimized synthetic DNA fragments encoding the two MOMP sequences were inserted into the *hbp* ORF using SacI/BamHI restriction sites.

Construction of a Δ*tolRA* mutant in *S.* Typhimurium. *S.* Typhimurium SL3261 Δ*tolRA* was constructed using the λ Red-mediated recombination system essentially as described by Datsenko and Wanner (39). Briefly, primers tolRASLHP1 (5′-TGC ACC GCC AGG CGT TTA CCG TAA GCG AAA GCA ACA AGG GGT AAG CCA TGA TTC CGG GGA TCC GTC GAC C-3′) and tolRASLHP2 (5′-ACT GCT CTA ACT TCC ATA AAG AAA AGT ATC TAC AGT TTA AAG TCT AGT TTG GCT GTA GGC TGG AGC TGC TTC G-3′) were used in combination with pKD13 to create a kanamycin cassette PCR product with suitable overhangs for recombination into the chromosome of SL3261. The PCR product was electroporated into SL3261 carrying the Red helper plasmid pKD46, allowing replacement of the *tolR* and *tolA* genes by Red-mediated recombination. The resulting strain was cured from the temperature-sensitive pKD46 by cultivation at 37°C. Insertion of the kanamycin cassette into the correct position on the chromosome was verified essentially as described by Baba and Mori (40) using the primers TolRAU (5′-CGT AAG CGA AAG CAA CAA GG-3′) and TolRAD (5′-CCA CCA GGA CCA GTA ACA AC-3′).

General protein production and analysis. The expression of ORFs encoding Hbp derivatives from pEH3 plasmids (38) was under the control of the *lacUV5* promoter. Strains harboring pEH3 vectors were grown until an optical density at 660 nm (OD_{660}) of ~0.3 (*E. coli*) or ~0.6 (*S.* Typhimurium), at which time expression of Hbp derivatives was induced in the presence of 50 μM or 1 mM isopropyl β-D-thiogalactopyranoside (IPTG) for 3 h for *E. coli* or of 50 or 100 μM IPTG for 1 h for *S.* Typhimurium. Bacteria were separated from spent medium by low-speed centrifugation, after which culture supernatants were treated with trichloroacetic acid to precipitate proteins or used to isolate OMVs as described below. Proteins were analyzed by SDS-PAGE, followed by staining with Coomassie G-250 (Bio-Rad) or immunoblotting. Immunostaining was performed with mouse monoclonal antibodies directed against ESAT6 (Hyb 76-8) (41), Ag85B$_C$ (TD17) (42), or RNA polymerase (W0003; NeoClone) or with rabbit polyclonal serum recognizing the Hbp passenger domain (J40)

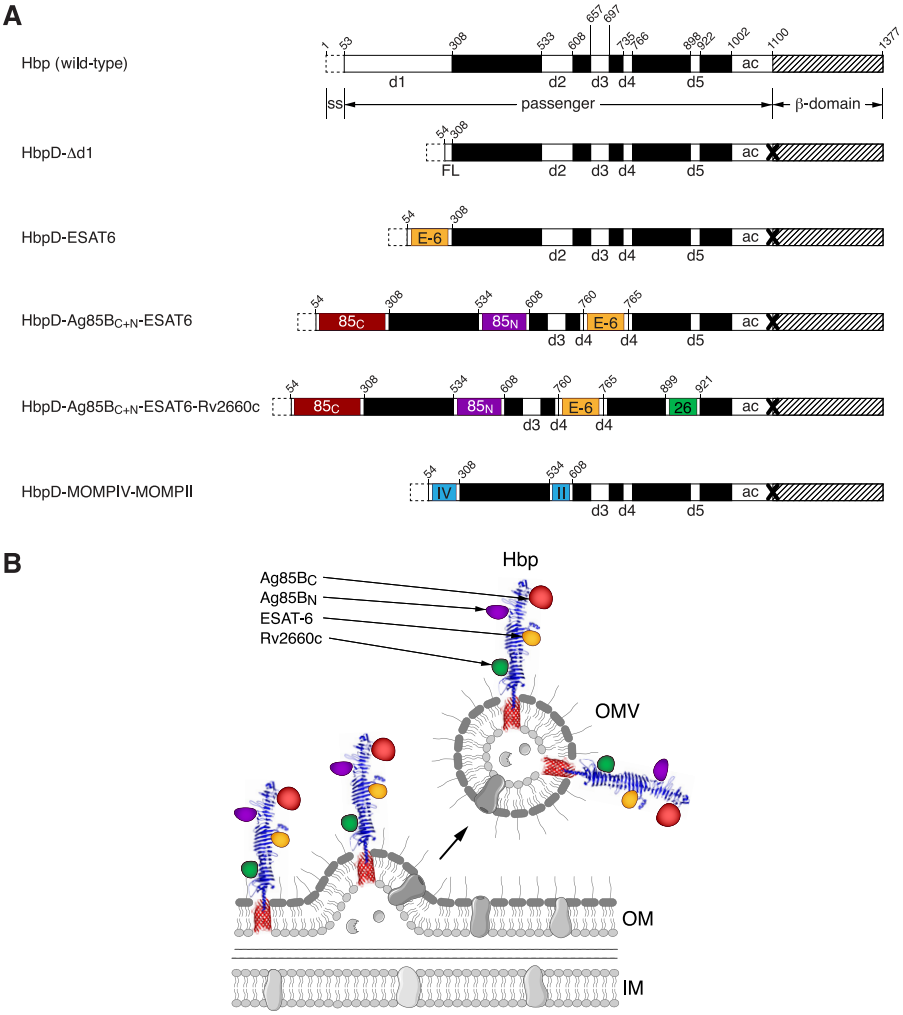

FIG 1 Hbp derivatives used for display at the OMV surface. (A) Wild-type Hbp (included for reference) is composed of three domains: (i) an N-terminal cleavable signal sequence (ss), (ii) a secreted passenger domain, and (iii) a C-terminal β-domain that becomes integrated into the OM. Side domains d1 to d5 and the autochaperone domain (ac) that is involved in OM translocation of the passenger domain are indicated, while the remainder of the passenger domain is black. The mutation that prevents autocatalytic intradomain cleavage and concomitant release of the passenger, resulting in a surface-exposed (display) version of Hbp, is marked X. Numbers above the diagrams correspond to the amino acid positions in wild-type Hbp. Insertion of a 9- to 11-aa flexible linker (FL) comprising Gly and Ser residues and insertions of the mycobacterial antigens ESAT6 (E-6), an N-terminal fragment (aa 1 to 126; 85_N) and a C-terminal (aa 118 to 285; 85_C) fragment of Ag85B, Rv2660c (26), and the internal fragments MOMPIV (aa 266 to 350; IV) and MOMPII (aa 155 to 190; II) of *C. trachomatis* MOMP are indicated. All inserts are flanked by short Gly/Ser linkers. (B) Schematic representation of Hbp-mediated antigen display on OMVs, exemplified by HbpD-Ag85B$_{C+N}$-ESAT6-Rv2660c. Ag85B, split into N-terminal and C-terminal fragments, ESAT6, and Rv2660c are fused to the Hbp passenger by replacement of side domains d2, d1, d4, and d5, respectively. Upon production in hypervesiculating *E. coli* or *Salmonella* strains, the Hbp chimera, which localizes in the bacterial outer membrane (OM), becomes incorporated in and displayed at the surface of the newly formed outer membrane vesicles (OMV). IM, inner membrane. The figure was made using Servier Medical Art and the crystal structures of the Hbp passenger (blue) and β-domain (red) (32, 66).

(43), the Hbp β-barrel (SN477) (44), *C. trachomatis* serovar D MOMP (I. Rosenkrands, Statens Serum Institut, Denmark), DnaJ (45), BamA (J. Tommassen, Utrecht University, The Netherlands), SurA (T. Silhavy, Princeton University, USA), Skp (46), leader peptidase (Lep), OmpA, SecG, or trigger factor (TF) (from our own laboratory collection), or with rat antiserum specific for Rv2660c (P. Andersen, Statens Serum Institut, Denmark). For quantitative Western blotting, secondary IRDye 680RD goat anti-rabbit IgGs (Li-Cor) were used, and fluorescent signals were detected with an Odyssey Infrared Imaging System (Li-Cor).

OMV isolation. Culture supernatants obtained by low-speed centrifugation were passed through 0.45-μm-pore-size filters (Millipore) and centrifuged at 208,000 × *g* for 60 min to separate OMVs from soluble proteins. The pelleted crude vesicles were resuspended in phosphate-buffered saline (PBS).

Velocity density gradient centrifugation was performed essentially as described previously (15). Briefly, the crude vesicle preparation was adjusted to 45% (vol/vol) OptiPrep density gradient medium (Axis Shield) in 400 μl and transferred to the bottom of a 12.5-ml ultracentrifuge tube. Subsequently, OptiPrep-PBS dilutions of 35% (3 ml), 30% (3 ml), 25% (2 ml), 20% (2 ml), 15% (1 ml), and 10% (1 ml) were layered in descending order atop the preceding layers. Gradients were centrifuged at 130,000 × *g* for 16 h, and fractions of equal volumes were collected sequentially from the top.

Proteinase K accessibility assay. OMVs were resuspended in a buffer containing 50 mM Tris-HCl (pH 7.4) and 1 mM $CaCl_2$. When required, OMVs were lysed by incubation with 0.5% (vol/vol) Triton X-100 (Sigma-Aldrich) for 15 min on ice. Intact and lysed OMVs were incubated for 30 min at 37°C in the presence of 100 μg/ml proteinase K (Roche Applied

Science). The reaction was stopped by the addition of 0.1 mM phenylmethanesulfonyl fluoride (Roche Applied Science), and all samples were precipitated with trichloroacetic acid.

Immunogold EM. Crude OMVs in PBS were fixed by addition of an equal volume of fixation solution (4% paraformaldehyde and 0.2% glutaraldehyde in 0.4 M PHEM buffer consisting of 240 mM PIPES [piperazine-*N*,*N*′-bis(2-ethanesulfonic acid)], 100 mM HEPES, 8 mM $MgCl_2$, and 40 mM EGTA, pH 6.9) and incubation for 2 h at room temperature. The fixed OMVs were pelleted by centrifugation at 280,000 × *g* for 20 min, after which they were resuspended in 0.1 M PHEM buffer containing 0.5% paraformaldehyde. Samples were transferred to a Formvar-coated copper grid, and immunolabeling was performed using antiserum recognizing the Hbp passenger (J40) (43), rabbit anti-mouse bridging serum (Dako), and protein A conjugated to a 10-nm gold particle. OMVs were stained with 2% uranyl acetate, and subsequent electron microscopy (EM) analysis was carried out using a CM 10 microscope (FEI).

Dynamic light scattering. The diameters of isolated OMVs were determined by dynamic light scattering using a Zetasizer instrument (Zetasizer Nano ZS; Malvern Instruments) as described previously (47). The dynamic light-scattering data were analyzed with the latest Zetasizer family software (version 7.04; Malvern Instruments) using the normal resolution analysis mode. All data met the quality criteria (polydispersity index lower than 0.3).

Mass spectrometric (MS) analysis. Protein bands were excised from Coomassie-stained SDS-PAGE gels and processed for in-gel digestion. Each gel slice was cut in pieces, washed with water, and destained in 50 mM ammonium bicarbonate (ABC)–50% (vol/vol) methanol. The slices were dehydrated in 50 mM ABC–50% (vol/vol) acetonitrile, followed by 100% acetonitrile, and dried in a vacuum centrifuge. Subsequently, the slices were rehydrated in 50 mM ABC containing 4.8 ng/μl Trypsin Gold (Promega) and 0.01% ProteaseMAX surfactant (Promega) for 1 h at 50°C. The trypsin was inactivated by the addition of 0.5% trifluoroacetic acid, after which the extracted tryptic peptides were dried in a vacuum centrifuge.

For tandem MS (MS/MS) analysis, the extracted peptides were concentrated and desalted on C_{18} ZipTips (Millipore), eluted in α-cyano-4-hydroxy-cinnamic acid matrix, and analyzed by matrix-assisted laser desorption ionization–two-stage time of flight (MALDI-TOF/TOF) MS (AB Sciex TOF/TOF 5800). An MS/MS spectrum search was performed against the *E. coli* K-12 MG1655 database using Mascot software (Matrix Science), with a peptide mass tolerance of 1.2 Da and a fragment mass tolerance of 0.6 Da and allowing a single site of miscleavage and oxidation of methionine as a variable modification.

For nanoscale liquid chromatography coupled to tandem mass spectrometry (nano-LC-MS/MS), the tryptic peptides were resuspended in 0.1% acetic acid, separated on a capillary C_{18} column using a nanoLC-1D Plus high-performance liquid chromatography (HPLC) system (Eksigent), and analyzed online with an electrospray linear trap quadrupole (LTQ)-Orbitrap Discovery mass spectrometer (Thermo Fisher Scientific). MS/MS searches were performed against the UniProt *E. coli* K-12 database using MaxQuant software (48) with a maximum peptide mass deviation of 6 ppm and a fragment mass deviation of 20 ppm, while allowing two sites of miscleavage and treating methionine oxidation and N-terminal acetylation as variable modifications. Proteins were quantified by spectral counting, and statistical testing was performed using the BetaBinominal test (49).

***In vitro* antigen presentation assay.** Bone marrow-derived dendritic cells (BMDCs) from C57BL/6 mice, generated in the presence of 2 ng/ml granulocyte-macrophage colony-stimulating factor, were incubated for 4 h with OMVs displaying Hbp (derivatives), purified Hbp-Ag85B$_{C+N}$-ESAT6-Rv2660c (200 μg/ml), or synthetic peptide consisting of residues 241 to 260 of Ag85A (Ag85A$_{241–260}$) or residues 1 to 20 of ESAT6 (ESAT6$_{1–20}$). Thereafter, the BMDCs were washed three times and cocultured overnight with C57BL/6-derived T cell hybridoma cells (DE10) (50) that recognize the 1-A^b-restricted Ag85A$_{241–260}$ peptide and cross-react with an I-A^b-restricted peptide in Ag85B (Ag85B$_{281–300}$). The presence of interleukin-2 (IL-2), produced upon antigen recognition, in the supernatant of cocultures was monitored by standard IL-2-specific enzyme-linked immunosorbent assay. All work involving animals was approved by the Pasteur Institute Safety Committee in accordance with French and European guidelines.

RESULTS

Hbp platform allows targeting of heterologous proteins to *E. coli* OMVs. We have recently shown that heterologous proteins can be efficiently displayed at the surface of *E. coli* and *S.* Typhimurium as fusion partners of the AT Hbp (26, 34), and we reasoned that Hbp might also be used to target proteins to OMVs (Fig. 1B). First, to establish that Hbp itself is targeted to OMVs, an ORF encoding an uncleaved (display) version of Hbp (Fig. 1A) that lacks side domain d1 (HbpD-Δd1) was expressed under the control of a *lac*-derived promoter in the hypervesiculating *E. coli* strain JC8031 (Δ*tolRA*) (36) in the presence of 50 μM IPTG. OMVs were separated from soluble secreted proteins in cell-free supernatants by ultracentrifugation, and the production of Hbp was monitored by SDS-PAGE and Coomassie staining. Successful enrichment of OMVs in the high-speed centrifugation pellet was confirmed by the presence of two bands of ~35 and ~32 kDa, which were verified by mass spectrometry (data not shown) to correspond to the major OMPs and OMV marker proteins OmpF/C and OmpA (4, 5) (Fig. 2A, lanes 16 to 20). As expected, HbpD-Δd1 accumulated as an ~116-kDa band in the whole-cell fraction (Fig. 2A, lane 2). Interestingly, in the culture supernatant a band of similar size was detected (Fig. 2A, lane 7), which in similarity to the porins was detected in the OMV fraction after ultracentrifugation (Fig. 2A, lane 17, and B, lane 2). Furthermore, upon velocity density gradient centrifugation of the crude vesicles, HbpD-Δd1 migrated to the same fractions as OmpA, -F, and -C (Fig. 2C). This confirms that the Hbp display variant is tightly associated and most likely integral to the OMVs. Of note, comparison of the ratios of Hbp and OmpA in OMVs and whole cells by quantitative Western blotting indicated that Hbp is neither enriched nor selectively excluded in the OMVs (not shown).

To investigate whether Hbp can target heterologous proteins to OMVs, three chimeric constructs containing one, two, or three *M. tuberculosis* antigens simultaneously (26; also Jong et al., unpublished) (Fig. 1) were produced in JC8031, and crude OMVs were isolated. In the first chimera, HbpD-ESAT6, d1 was replaced by the 9.9-kDa antigen ESAT6 (26). In the second chimera, HbpD-Ag85B$_{C+N}$-ESAT6, two fragments corresponding to the N-terminal (residues 1 to 126) and the C-terminal (residues 118 to 285) portions of the mature 31-kDa protein Ag85B replaced d2 and d1, respectively, and ESAT6 was fused to the position corresponding to d4. In the third chimera, HbpD-Ag85B$_{C+N}$-ESAT6-Rv2660c, the full-length 7.6-kDa Rv2660c protein was additionally inserted via substitution of d5 (Jong et al., unpublished). Importantly, all three chimeras were detected in the OMV fraction upon protein staining (Fig. 2A) and by immunoblotting (Fig. 2B). Furthermore, HbpD-ESAT6 was shown to migrate to the same fractions as OmpF/C and OmpA upon velocity density gradient centrifugation, verifying its presence in the OMVs (Fig. 2D). A minor band migrating just below the ~126-kDa full-length HbpD-ESAT6 chimera was also detected (Fig. 2A, lane 18, and 2B, lane 3), which represents a previously observed product that probably results from proteolytic cleavage of the passenger (26). Of

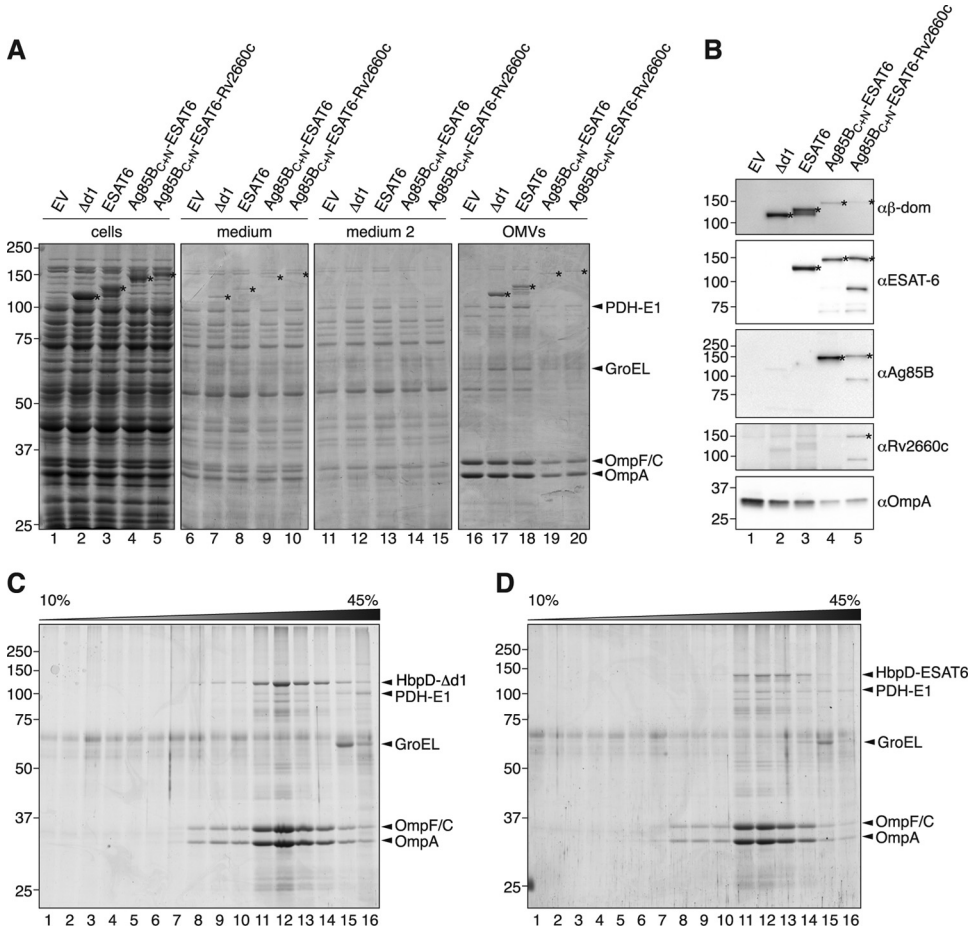

FIG 2 Targeting of (multiple) heterologous proteins to *E. coli* OMVs by fusion to the passenger of Hbp. (A) SDS-PAGE/Coomassie analysis of fractions containing an equivalent of 0.1 OD_{660} unit of cells, culture medium, secreted soluble proteins (medium 2), and 3 OD_{660} units of crude OMVs from *E. coli* JC8031 expressing HbpD-Δd1, HbpD-ESAT6, HbpD-Ag85B$_{C+N}$-ESAT6, and HbpD-Ag85B$_{C+N}$-ESAT6-Rv2660c in the presence of 50 μM IPTG or harboring the empty vector (EV). Hbp proteins (chimeras) are marked by asterisks, and arrowheads indicate the bands corresponding to PDH-E1, GroEL, OmpF/C, and OmpA. (B) The OMV samples from panel A were analyzed by immunoblotting using antibodies recognizing the β-domain of Hbp (αβ-dom), ESAT6, Ag85B, Rv2660c, and OmpA. (C and D) SDS-PAGE/Coomassie analysis of equal volumes of all fractions obtained after velocity density gradient centrifugation of crude OMVs containing HbpD-Δd1(C) or HbpD-ESAT6 (D). The concentration of OptiPrep (%) and bands corresponding to HbpD-Δd1, HbpD-ESAT6, PDH-E1, GroEL, OmpF/C, and OmpA are indicated. α, anti.

note, the levels of OMV production appeared to be slightly affected upon expression of the two most complex Hbp chimeras, as judged by the levels of the porins OmpF/C and OmpA (Fig. 2A, lanes 19 to 20, and 2B, lanes 4 to 5). Nevertheless, together the results show that the Hbp platform allows efficient targeting of multiple heterologous proteins simultaneously to *E. coli* OMVs.

Hbp-antigen fusions are displayed at the surface of *E. coli* OMVs. Hbp naturally undergoes an autocatalytic cleavage mechanism after translocation across the OM, resulting in release of the passenger from the β-domain (33, 35). We previously created an uncleaved version of Hbp by mutating the intradomain cleavage site, in which the exported passenger remains covalently attached to the β-domain and is exposed at the bacterial surface (34). To determine if Hbp is exposed at the OMV surface as well, the localization of HbpD-Δd1 was analyzed by immunogold labeling and EM. OMVs from *E. coli* JC8031 producing HbpD-Δd1 were labeled with Hbp-specific antibodies (Fig. 3A), whereas no labeling was observed of OMVs derived from the strain harboring the empty vector (Fig. 3B). The EM analysis also showed that both the Hbp-containing vesicles and the empty vesicles were closed, spherical particles. Furthermore, dynamic light-scattering analysis (Fig. 3C) showed that the OMVs isolated from the strain harboring the empty vector had a diameter of 47.7 nm ± 12.6 nm ($n = 2$), similar to what has been observed previously with this strain (14). Importantly, vesicles isolated from the HbpD-Ag85B$_{C+N}$-ESAT6-Rv2660c-expressing strain were very similar in size (47.5 nm ± 13.5 nm; $n = 2$).

To determine whether Hbp display constructs containing heterologous inserts are also targeted to the OMV surface, we incubated intact OMVs producing HbpD-Δd1, HbpD-ESAT6, HbpD-Ag85B$_{C+N}$-ESAT6, and HbpD-Ag85B$_{C+N}$-ESAT6-Rv2660c with proteinase K. This treatment resulted in the degradation of all four display constructs, as demonstrated by SDS-PAGE and Coomassie staining (Fig. 4A) and by immunoblotting (data not shown). OmpA, which has a protease-sensitive periplasmic domain at the C terminus, appeared degraded only after permeabilization of the OMVs with Triton X-100 (Fig. 4A). This confirmed the integrity and the membrane orientation of the OMVs. The integral mem-

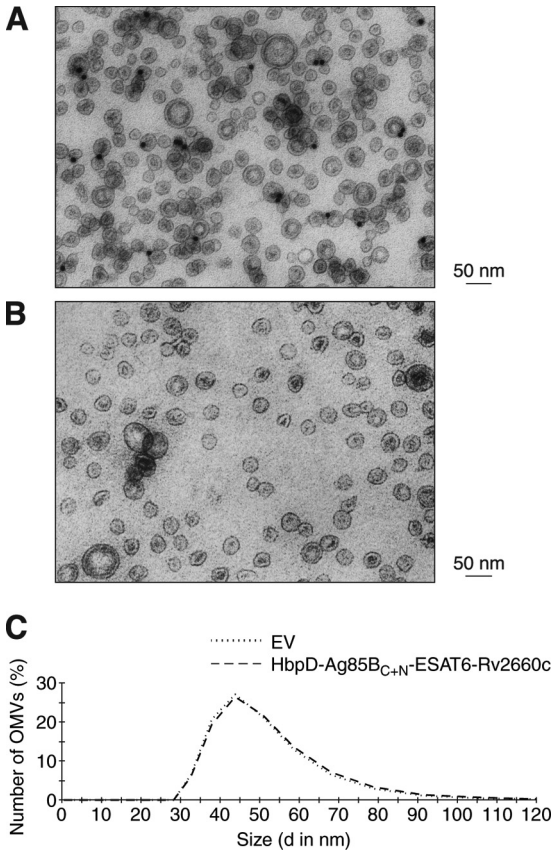

FIG 3 Surface labeling, shape, and size of *E. coli* OMVs containing Hbp (chimeras). (A and B) Intact OMVs isolated from JC8031 producing HbpD-Δd1 (A) or harboring the empty vector (B) were fixed and probed with anti-Hbp antibodies, followed by 10-nm gold-labeled secondary antibodies, and analyzed by electron microscopy. Scale bar, 50 nm. (C) Representative curves of the size distribution for OMVs isolated from JC8031 carrying the empty vector (EV) or producing HbpD-Ag85B$_{C+N}$-ESAT6-Rv2660c, analyzed by number. d, diameter.

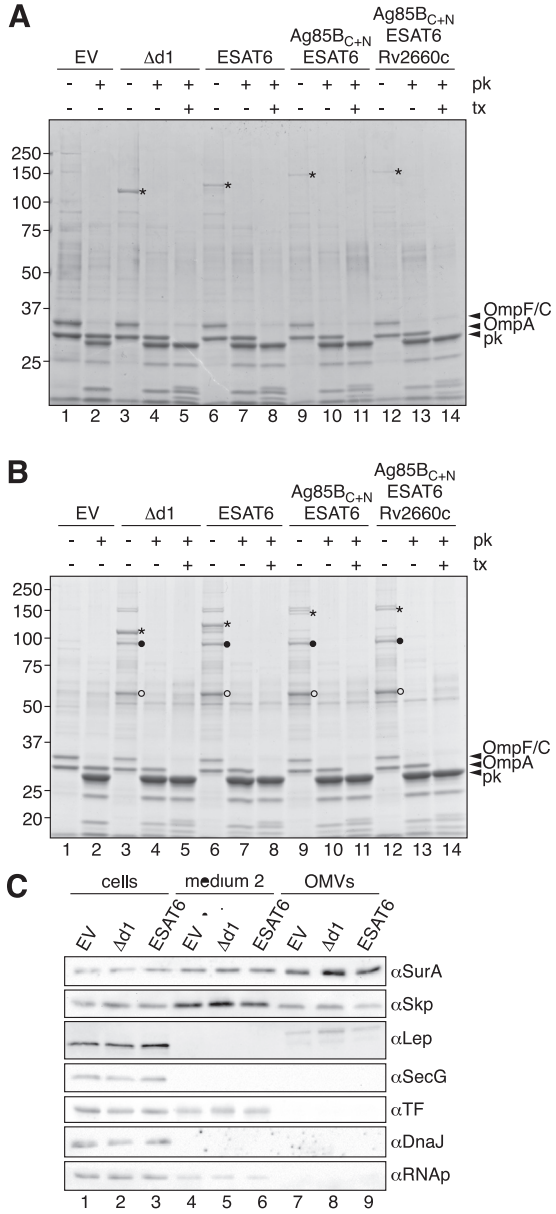

FIG 4 Surface localization and effect on vesicle protein composition of Hbp (chimeras) in *E. coli* OMVs. (A and B) Equal amounts of intact OMVs (−tx) or OMVs permeabilized with Triton X-100 (+tx) from *E. coli* JC8031 harboring the empty vector (EV) or producing Hbp display constructs (described in the legend of Fig. 1) in the presence of 50 μM (A) or 1 mM (B) IPTG were incubated with proteinase K (+pk) or mock treated (−pk), separated by SDS-PAGE, and stained with Coomassie. Asterisks, Hbp (chimeras); filled circles, PDH-E1; open circles, GroEL, arrowheads, OmpF/C, OmpA, and proteinase K. (C) Immunoblot analysis of fractions containing an equivalent of 0.1 OD unit of whole cells, 0.1 OD unit of soluble material (medium 2), or 3 OD units of insoluble material (OMVs) obtained after ultracentrifugation of cell-free culture supernatants from *E. coli* JC8031 cells harboring the empty vector or producing HbpD-Δd1 or HbpD-ESAT6. The periplasmic proteins SurA and Skp, the inner membrane proteins Lep and SecG, and the cytoplasmic proteins TF, DnaJ, and RNA polymerase were detected with specific antibodies.

brane proteins OmpF/C were also susceptible to proteinase K treatment (Fig. 4A), which is likely because the loops in these β-barrel proteins are (partly) exposed at the surface of the *E. coli* OMVs.

Taken together, the results show that Hbp can be used to efficiently decorate the surface of *E. coli* OMVs with antigens, without altering the size, shape, or orientation of the OMVs.

Effect of Hbp expression on OMV protein composition. Although OmpF/C, OmpA, and Hbp (chimeras) were the most abundant proteins, we noticed that our OMV preparations contained two additional bands of ~60 and ~90 kDa upon expression of Hbp (derivatives) (Fig. 2A). These bands became more prominent upon higher levels of Hbp expression (Fig. 4B shows results of induction with 1 mM IPTG). The two bands were determined by mass spectrometry to correspond to the cytoplasmic proteins GroEL and pyruvate dehydrogenase E1 (PDH-E1) (data not shown). Importantly, immunoblotting showed that our OMVs contained the periplasmic proteins SurA and Skp but not the IM proteins SecG and Lep nor the cytoplasmic proteins TF, DnaJ, and RNA polymerase (Fig. 4C). Therefore, we could rule out that the presence of GroEL and PDH-E1 in our OMVs was a result of generic contamination with cytoplasmic material. Furthermore, GroEL and PDH-E1 are not integrated in the vesicles but probably loosely associated with the OMV surface since they were both degraded upon treatment of intact OMVs with proteinase K (Fig. 4B). In addition, GroEL and, to some extent, also

TABLE 1 Proteins downregulated in *E. coli* OMVs upon production of Hbp-Δd1 or HbpD-ESAT6

UniProt accession no.	Gene name	Description	Mol mass (kDa)	Spectral count			Expression in OMVs containing: HbpD-Δd1		HbpD-ESAT6	
				EV	HbpD-Δd1	HbpD-ESAT6	Fold change[a]	*P* value	Fold change[a]	*P* value
P07024	*ushA*	Protein UshA	61	6	0	1	∞	0.024	−5.6	0.072
P09394	*glpQ*	Glycerophosphoryl diester phosphodiesterase	41	5	0	0	∞	0.028	∞	0.031
P05458	*ptrA*	Protease 3	108	4	0	0	∞	0.036	∞	0.039
P33363	*bglX*	Periplasmic beta-glucosidase	83	10	1	1	−11.1	0.024	−9.3	0.028
P23847	*dppA*	Periplasmic dipeptide transport protein	60	90	9	9	−9.9	0.002	−10.3	0.002
P0A6F5	*groEL*	60-kDa chaperonin	57	7	1	10	−7.8	0.042	1.4	0.518
P08331	*cpdB*	2,3-Cyclic nucleotide 2-phosphodiesterase/3-nucleotidase	71	5	1	0	−5.6	0.080	∞	0.031
P45523	*fkpA*	FKBP-type peptidyl-prolyl *cis-trans* isomerase FkpA[b]	29	20	7	10	−2.8	0.036	−2.1	0.076
P0ADS6	*yggE*	Uncharacterized protein YggE	27	23	13	9	−1.8	0.084	−2.7	0.036
P31554	*lptD*	LPS assembly protein LptD	90	39	22	16	−1.8	0.052	−2.4	0.026
P0C0V0	*degP*	Periplasmic serine endoprotease DegP	49	61	42	29	−1.5	0.072	−2.1	0.021
P02930	*tolC*	Outer membrane protein TolC	54	82	56	45	−1.5	0.045	−1.8	0.020
P45464	*lpoA*	Penicillin-binding protein activator LpoA	73	86	57	48	−1.5	0.039	−1.8	0.021
P0A855	*tolB*	Protein TolB	46	71	47	41	−1.5	0.050	−1.7	0.031
P0A940	*bamA*	Outer membrane protein assembly factor BamA	91	140	98	101	−1.4	0.030	−1.4	0.040
P06959	*aceF*	Dihydrolipoyllysine residue acetyltransferase component of pyruvate dehydrogenase complex	66	224	187	165	−1.2	0.072	−1.4	0.025

[a] Fold change in the OMVs containing either HbpD-Δd1 or HbpD-ESAT6 compared to the empty vector (EV) control OMVs.
[b] FKBP, FK506-binding protein.

PDH-E1 were separated from the porins OmpF/C and OmpA upon velocity density gradient centrifugation (Fig. 2C and D).

To further investigate the influence of the expression of Hbp (derivatives) on the OMV protein composition, OMVs purified by velocity density gradient centrifugation (Fig. 2C and D) were subjected to nano-LC-MS/MS. Of note, because a small number of peptides corresponding to GroEL were (differentially) detected (Table 1), we cannot rule out that the purified OMVs were contaminated with small amounts of nonintegral or lumenal vesicle proteins. Nevertheless, the analysis revealed only minor differences between OMVs containing HbpD-Δd1 or HbpD-ESAT6 and those produced by the strain harboring the empty vector (Tables 1 and 2). Most notably, expression of HbpD-Δd1 or HbpD-ESAT6 led to the incorporation of OsmB, a slight upregulation of OmpX and MipA (Table 2), and downregulation of a limited number of periplasmic and OM proteins, including BglX and DppA, in the OMVs (Table 1). As overexpression of heterologous secretory proteins is known to saturate the Sec machinery capacity, it is possible that this downregulation is the result of competition with overproduced Hbp at the Sec translocon in the IM (51). In conclusion, these results indicate that targeting of Hbp (derivatives) to *E. coli* OMVs has only a minor effect on the integral and lumenal OMV protein composition.

Construction of a hypervesiculating *S.* Typhimurium mutant. We have recently demonstrated that our Hbp platform can be used to secrete and display heterologous proteins at the surface of the attenuated *S.* Typhimurium SL3261 vaccine strain (26). Because OMVs offer an interesting alternative to live vaccines, we were interested in generating *Salmonella* OMVs displaying such antigens. First, to increase the OMV production level, a derivative of *S.* Typhimurium SL3261 was constructed in which the *tolR* and *tolA* genes were deleted by replacement with a kanamycin cassette. Proper deletion was verified by PCR. Upon analysis by SDS-PAGE and Coomassie staining, two clear bands corresponding to *Salmonella* OmpF/C and OmpA were detected in a culture supernatant of the mutant strain (Fig. 5A). This confirmed that inactivation of *tolRA* resulted in OMV overproduction in *S.* Typhimurium, similar to the hypervesiculating *E. coli* strain JC8031.

TABLE 2 Proteins upregulated in *E. coli* OMVs upon production of Hbp-Δd1 or HbpD-ESAT6

UniProt accession no.	Gene name	Description	Mol mass (kDa)	Spectral count			Expression in OMVs containing: HbpD-Δd1		HbpD-ESAT6	
				EV	Hbp-Δd1	HbpD-ESAT6	Fold change[a]	*P* value	Fold change[a]	*P* value
P0ADA7	*osmB*	Osmotically inducible lipoprotein B	7	0	12	7	∞	0.013	∞	0.024
P22525	*ycbB*	Probable L,D-transpeptidase YcbB	68	0	5	1	∞	0.031	∞	0.227
P76115	*yncD*	Probable TonB-dependent receptor YncD	77	0	4	5	∞	0.040	∞	0.029
P0A7R5	*rpsJ*	30S ribosomal protein S10	12	0	3	4	∞	0.058	∞	0.036
P0A917	*ompX*	Outer membrane protein X	19	150	456	435	3.0	0.001	2.9	0.001
P0A908	*mipA*	MltA-interacting protein	28	16	44	51	2.7	0.016	3.2	0.011
P06996	*ompC*	Outer membrane protein C	40	364	372	436	1.0	0.758	1.2	0.034

[a] Fold change in the OMVs containing either HbpD-Δd1 or HbpD-ESAT6 compared to the empty vector (EV) control OMVs.

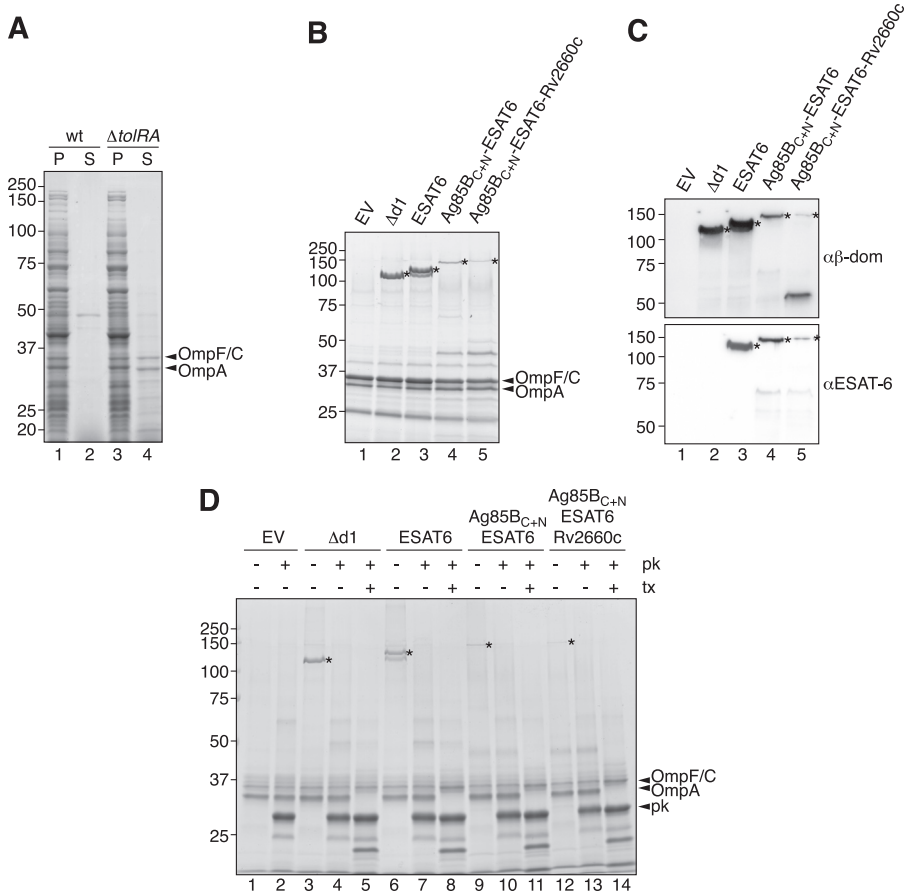

FIG 5 Display of *M. tuberculosis* antigens at the surface of OMVs derived from an OMV-overproducing strain of *S.* Typhimurium. (A) SDS-PAGE/Coomassie analysis of an equivalent of 0.05 OD_{660} unit of cell pellets (P) and 10-fold more culture supernatants (S) from *S.* Typhimurium SL3261 (wt) and an isogenic OMV-overproducing mutant constructed by deletion of *tolR* and *tolA* (Δ*tolRA*). (B and C) Crude OMVs isolated from SL3261 Δ*tolRA* producing Hbp (chimeras) in the presence of 100 μM IPTG (HbpD-Δd1 and HbpD-ESAT6) or 50 μM IPTG (HbpD-Ag85B$_{C+N}$-ESAT6 and HbpD-Ag85B$_{C+N}$-ESAT6-Rv2660c) or harboring the empty vector (EV) were separated by SDS-PAGE and analyzed by Coomassie-staining (B) and immunoblotting using antibodies specific for the β-domain of Hbp (αβ-dom) and ESAT6 (C). (D) Proteinase K accessibility of OMVs described in panels B and C. Equivalent amounts of intact OMVs (−tx) or OMVs permeabilized with Triton X-100 (+tx), were incubated with proteinase K (+pk) or mock treated (−pk) and analyzed by SDS-PAGE/Coomassie staining. Full-length Hbp species are marked with asterisks, and OmpF/C, OmpA, and proteinase K are indicated with arrowheads.

Display of *M. tuberculosis* antigens at the surface of *Salmonella* OMVs. To investigate whether Hbp derivatives are targeted to *Salmonella* OMVs, HbpD-Δd1 and Hbp-antigen fusions were produced in SL3261 Δ*tolRA*, and crude OMVs were isolated as described for the *E. coli* OMVs. As shown by protein staining upon SDS-PAGE (Fig. 5B) and immunoblotting (Fig. 5C), the various chimeras, similar to OmpF/C and OmpA, were detected in the OMV preparations. As observed in *E. coli*, OMV production was slightly affected upon expression of the most complex constructs, HbpD-Ag85B$_{C+N}$-ESAT6 and HbpD-Ag85B$_{C+N}$-ESAT6-Rv2660c, as judged by the levels of porins detected (Fig. 5B, lanes 4 and 5). Importantly, treatment of intact OMVs with proteinase K demonstrated that all the chimeras were accessible at the surface of the *Salmonella* OMVs (Fig. 5D). Periplasmic OmpA was not degraded unless the vesicles were lysed by treatment with Triton X-100, indicating that the vesicles remained intact during the treatment. The band corresponding to OmpF/C was unaffected by the protease treatment, indicating that, in contrast to *E. coli*, the external loops of these proteins are not accessible at the surface of the *Salmonella* OMVs. In conclusion, efficient surface display of multiple heterologous proteins at the surface of *Salmonella* OMVs was achieved by combining the Hbp display platform with the newly constructed *S.* Typhimurium SL3261 Δ*tolRA* mutant strain.

Display of epitopes from *C. trachomatis* MOMP on *Salmonella* OMVs. The immunodominant major outer membrane protein of *C. trachomatis* is considered an attractive target for development of a subunit vaccine against chlamydial disease. This cysteine-rich protein inserts into the chlamydial OM in a β-barrel conformation, but attempts at recombinant MOMP production typically fail due to misfolding and aggregation (52). To avoid these problems, we decided to express immunogenic fragments of MOMP as fusions to Hbp. In a single Hbp carrier molecule, d1 and d2 were replaced by fragments corresponding to aa 266 to 350 and aa 155 to 190 of MOMP, respectively (Jong et al., unpublished). These fragments, respectively, encode the surface-exposed variable sequences (VS) VS4 and VS2 of MOMP, which contain structural B cell epitopes (53), and adjacent intracellular sequences that are enriched in conserved $CD4^+$ and $CD8^+$ T cell epitopes (54). Upon production in *S.* Typhimurium SL3261 Δ*tolRA*, the HbpD-MOMPIV-MOMPII chimera was directed to

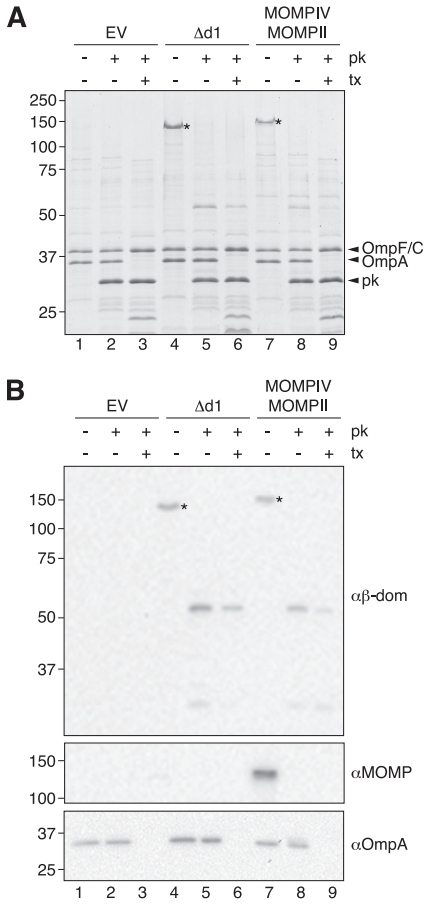

FIG 6 Display of *C. trachomatis* MOMP fragments at the surface of *Salmonella* OMVs. Equivalent amounts of OMVs isolated from *S.* Typhimurium SL3261 Δ*tolRA* producing HbpD-Δd1 or HbpD-MOMPIV-MOMPII in the presence of 100 μM IPTG or carrying the empty vector (EV) were left intact (−tx) or permeabilized with Triton X-100 (+tx), prior to incubation with proteinase K (+pk) or mock treatment (−pk). Samples were analyzed by SDS-PAGE/Coomassie staining (A) and immunoblotting using antiserum recognizing the β-domain of Hbp (αβ-dom), MOMP, and OmpA (B). Full-length Hbp species are marked with asterisks, and OmpF/C, OmpA, and proteinase K are indicated with arrowheads.

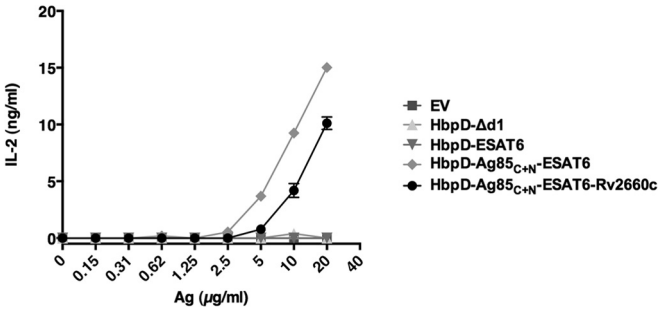

FIG 7 Processing and presentation of *M. tuberculosis* antigens displayed at the surface of *S.* Typhimurium OMVs to the MHC class II pathway. C57BL/6 (H-2^b) BMDCs were incubated with OMVs isolated from *S.* Typhimurium SL3261 Δ*tolRA* producing Hbp (chimeras) or harboring the empty vector (EV). The OMVs were added at different dilutions, expressed as the concentration of Hbp-antigen fusion (Ag) in the vesicle preparations. The BMDCs were washed and incubated with I-A^b-restricted $Ag85B_{281–300}$-specific DE10 T cell hybridoma cells. The production of IL-2 was measured by enzyme-linked immunosorbent assay. The results are presented as means of two replicates ± standard deviations (error bars) and are representative of three experiments.

the surface of the derived OMVs and were, as such, accessible to added proteinase K (Fig. 6). Strikingly, the efficiency of display was similar to that of HbpD-Δd1 (Fig. 6), underscoring the versatility of the Hbp platform.

Efficient processing and MHC class II-restricted presentation of Ag85B displayed at the surface of *Salmonella* OMVs. The mycobacterial proteins Ag85B and ESAT6 are potent T cell antigens (55). To determine whether antigen delivery by *S.* Typhimurium OMVs leads to proper processing and presentation of the exogenously inserted T cell epitopes, we took an *in vitro* approach. OMVs with surface-exposed Hbp chimeras were incubated with murine BMDCs to allow antigen uptake and processing. After removal of external OMVs by extensive washing, the BMDCs were cocultured with DE10 T cell hybridoma cells that specifically recognize an $Ag85A_{241–260}$ peptide that is restricted by the murine major histocompatibility complex (MHC) class II molecule I-A^b (50). Importantly, the DE10 cells also recognize a highly similar I-A^b-restricted peptide in Ag85B, i.e., $Ag85B_{281–300}$. Production of IL-2 showed that the DE10 hybridoma cells recognized appropriate histocompatible BMDCs that had been incubated with OMVs exposing HbpD-$Ag85B_{C+N}$-ESAT6 and HbpD-$Ag85B_{C+N}$-ESAT6-Rv2660c at the surface. In contrast, no IL-2 production was observed after incubation with BMDCs that had been exposed to OMVs displaying HbpD-Δd1, HbpD-ESAT6, or the empty vector control (Fig. 7). Production of IL-2 in response to the synthetic $Ag85A_{241–260}$ peptide, but not to an unrelated peptide control, confirmed the specificity of the DE10 hybridoma cells (data not shown). In addition, incubation of the hybridoma cells with the purified HbpD-$Ag85B_{C+N}$-ESAT6-Rv2660c fusion protein and increasing concentrations of OMVs confirmed that the antigen-specific IL-2 production was not affected by toxicity of the OMVs toward the BMDCs or the hybridoma cells (data not shown). These data show that delivery of the *S.* Typhimurium OMVs to DCs *in vitro* leads to correct and efficient processing and presentation of an immunodominant Ag85B $CD4^+$ T cell epitope that can be recognized by *M. tuberculosis*-specific T cells.

DISCUSSION

This work demonstrates that the Hbp autotransporter platform enables efficient targeting of heterologous proteins to the surface of *E. coli* and *Salmonella* OMVs. Targeting of heterologous polypeptides to *E. coli* or *Salmonella* OMVs has previously been studied in detail upon fusion to the N and C termini of the vesicle-associated toxin ClyA (21) and to the β-barrel of the autotransporter AIDA (22). However, detection of Hbp chimeras at the Coomassie level highlights the remarkable efficiency of the Hbp system compared to these previous approaches. Despite the fact that it was not enriched in the OMVs compared to the *E. coli* OM, Hbp was one of the major proteins detected in both *E. coli* and *Salmonella* OMVs. Furthermore, and in contrast to previous work, the side domain replacement strategy allows incorporation of multiple heterologous sequences in the same display module, demonstrating for the first time the simultaneous display of multiple antigens at the OMV surface (Fig. 1B).

Importantly, overexpression of Hbp had no major influence on the OMVs as no major changes in the size or morphology were detected, and only little variation was observed in the protein

composition of the OMVs isolated from the *E. coli* strain producing Hbp compared to those from the control strain. The most striking difference was the presence of GroEL and PDH-E1 in OMVs carrying Hbp (derivatives). This was somewhat surprising, considering that cytoplasmic and IM proteins are generally not present or are present only at very low levels in OMVs (4, 56). However, GroEL and members of the PDH complex have frequently been detected by proteomics in OMV preparations (57–60). Our analyses showed that GroEL and PDH-E1 were loosely associated with the OMV surface. Furthermore, OMV-associated GroEL was detected as an ~700-kDa complex upon blue native PAGE (data not shown), consistent with its cytoplasmic tetradecameric form (61). Therefore, and given their frequent association with OMVs and bacterial surfaces (57–60, 62), it is likely that GroEL and PDH-E1 leak from cells under stress conditions and reassociate with bacterial outer membranes or vesicles. Indeed, mild stress could be triggered by the overexpression of Hbp, a notion that is supported by the concomitant upregulation of the outer membrane lipoprotein OsmB, which is encoded by a multistress-responsive gene (63), and of OmpX, which is also known to respond to stress conditions (64). Finally, it should be noted that the overall levels of OMV production appeared slightly reduced upon expression of Hbp fused to three or four antigenic fragments. Although no striking differences were observed by general protein staining, we cannot rule out additional effects on the composition of the OMVs upon expression of more complex fusion proteins.

The robust display of three mycobacterial antigens, individually or simultaneously, at the surface of *E. coli* and *Salmonella* vesicles demonstrates the versatility of the Hbp platform. This versatility is further underscored using a fusion between Hbp and two immunogenic fragments of the *C. trachomatis* MOMP. This chimera was displayed at the surface of *Salmonella* OMVs with an outstanding efficiency, offering an alternative approach to the notoriously difficult recombinant production of MOMP. The advantage of combining multiple antigens in the same vaccine was previously described as immunization with an Ag85B-ESAT6-Rv2660c fusion protein promoted stronger immune responses and better protection against *M. tuberculosis* challenge in mice than vaccines based on the individual antigens (65). Efficient processing and presentation of OMV-associated Ag85B to the MHC class II pathway upon delivery to dendritic cells further highlight the applicability of our system for OMV vaccine development. Indeed, our preliminary data indicate that mice immunized intranasally with OMVs displaying HbpD-Ag85B$_{C+N}$-ESAT6-Rv2660c produce pulmonary vaccine-induced CD4$^+$ T cell responses, further emphasizing the potential of our approach for the development of recombinant OMV vaccines (Jong et al., unpublished).

ACKNOWLEDGMENTS

The research leading to these results has received funding from the European Union's Seventh Framework Programme (FP7/2007-2013) under grant agreement number 280873 ADITEC. In addition, W.S.P.J. was supported by a grant from the Dutch Technology Foundation, and Z.S. was supported by a Mosaic Grant from the Netherlands Organization for Scientific Research.

We thank G. Koningstein and R. C. van der Schors for technical assistance with the mass spectrometry, J. Tommassen, T. Silhavy, I. Rosenkrands, and P. Andersen for providing antisera, and S. Wagner for helpful discussions.

M.H.D.-S., C.M.T.H.-J., W.S.P.J., and J.L. are involved in Abera Bioscience AB, which aims to exploit the Hbp platform for vaccine development. D.V. and J.-W.D.G. are involved in Xbrane Bioscience AB. Abera Bioscience AB and Xbrane Bioscience AB are both part of Serendipity Innovations.

REFERENCES

1. **Beveridge TJ.** 1999. Structures of gram-negative cell walls and their derived membrane vesicles. J. Bacteriol. **181:**4725–4733.
2. **Bonnington KE, Kuehn MJ.** 2014. Protein selection and export via outer membrane vesicles. Biochim. Biophys. Acta **1843:**1612–1619. http://dx.doi.org/10.1016/j.bbamcr.2013.12.011.
3. **Schwechheimer C, Sullivan CJ, Kuehn MJ.** 2013. Envelope control of outer membrane vesicle production in Gram-negative bacteria. Biochemistry **52:**3031–3040. http://dx.doi.org/10.1021/bi400164t.
4. **Horstman AL, Kuehn MJ.** 2000. Enterotoxigenic *Escherichia coli* secretes active heat-labile enterotoxin via outer membrane vesicles. J. Biol. Chem. **275:**12489–12496. http://dx.doi.org/10.1074/jbc.275.17.12489.
5. **Kato S, Kowashi Y, Demuth DR.** 2002. Outer membrane-like vesicles secreted by *Actinobacillus actinomycetemcomitans* are enriched in leukotoxin. Microb. Pathog. **32:**1–13. http://dx.doi.org/10.1006/mpat.2001.0474.
6. **Wensink J, Witholt B.** 1981. Outer-membrane vesicles released by normally growing *Escherichia coli* contain very little lipoprotein. Eur. J. Biochem. **116:**331–335. http://dx.doi.org/10.1111/j.1432-1033.1981.tb05338.x.
7. **Brandtzaeg P, Bryn K, Kierulf P, Ovstebo R, Namork E, Aase B, Jantzen E.** 1992. Meningococcal endotoxin in lethal septic shock plasma studied by gas chromatography, mass-spectrometry, ultracentrifugation, and electron microscopy. J. Clin. Invest. **89:**816–823. http://dx.doi.org/10.1172/JCI115660.
8. **Hynes SO, Keenan JI, Ferris JA, Annuk H, Moran AP.** 2005. Lewis epitopes on outer membrane vesicles of relevance to *Helicobacter pylori* pathogenesis. Helicobacter **10:**146–156. http://dx.doi.org/10.1111/j.1523-5378.2005.00302.x.
9. **Li Z, Clarke AJ, Beveridge TJ.** 1998. Gram-negative bacteria produce membrane vesicles which are capable of killing other bacteria. J. Bacteriol. **180:**5478–5483.
10. **McBroom AJ, Kuehn MJ.** 2007. Release of outer membrane vesicles by Gram-negative bacteria is a novel envelope stress response. Mol. Microbiol. **63:**545–558. http://dx.doi.org/10.1111/j.1365-2958.2006.05522.x.
11. **Wai SN, Lindmark B, Soderblom T, Takade A, Westermark M, Oscarsson J, Jass J, Richter-Dahlfors A, Mizunoe Y, Uhlin BE.** 2003. Vesicle-mediated export and assembly of pore-forming oligomers of the enterobacterial ClyA cytotoxin. Cell **115:**25–35. http://dx.doi.org/10.1016/S0092-8674(03)00754-2.
12. **Yoon H, Ansong C, Adkins JN, Heffron F.** 2011. Discovery of *Salmonella* virulence factors translocated via outer membrane vesicles to murine macrophages. Infect. Immun. **79:**2182–2192. http://dx.doi.org/10.1128/IAI.01277-10.
13. **Alaniz RC, Deatherage BL, Lara JC, Cookson BT.** 2007. Membrane vesicles are immunogenic facsimiles of *Salmonella typhimurium* that potently activate dendritic cells, prime B and T cell responses, and stimulate protective immunity in vivo. J. Immunol. **179:**7692–7701. http://dx.doi.org/10.4049/jimmunol.179.11.7692.
14. **Bernadac A, Gavioli M, Lazzaroni JC, Raina S, Lloubes R.** 1998. *Escherichia coli tol-pal* mutants form outer membrane vesicles. J. Bacteriol. **180:**4872–4878.
15. **Chutkan H, Macdonald I, Manning A, Kuehn MJ.** 2013. Quantitative and qualitative preparations of bacterial outer membrane vesicles. Methods Mol. Biol. **966:**259–272. http://dx.doi.org/10.1007/978-1-62703-245-2_16.
16. **Gaillard ME, Bottero D, Errea A, Ormazabal M, Zurita ME, Moreno G, Rumbo M, Castuma C, Bartel E, Flores D, van der Ley P, van der Ark A, Hozbor DF.** 2014. Acellular pertussis vaccine based on outer membrane vesicles capable of conferring both long-lasting immunity and protection against different strain genotypes. Vaccine **32:**931–937. http://dx.doi.org/10.1016/j.vaccine.2013.12.048.
17. **Zollinger WD, Donets MA, Schmiel DH, Pinto VB, Labrie JE, III, Moran EE, Brandt BL, Ionin B, Marques R, Wu M, Chen P, Stoddard MB, Keiser PB.** 2010. Design and evaluation in mice of a broadly protective meningococcal group B native outer membrane vesicle vaccine. Vaccine **28:**5057–5067. http://dx.doi.org/10.1016/j.vaccine.2010.05.006.

18. **Granoff DM.** 2010. Review of meningococcal group B vaccines. Clin. Infect. Dis. **50**(Suppl 2)**:**S54–S65. http://dx.doi.org/10.1086/648966.
19. **Kesty NC, Kuehn MJ.** 2004. Incorporation of heterologous outer membrane and periplasmic proteins into *Escherichia coli* outer membrane vesicles. J. Biol. Chem. **279:**2069–2076. http://dx.doi.org/10.1074/jbc.M307628200.
20. **Muralinath M, Kuehn MJ, Roland KL, Curtiss R, III.** 2011. Immunization with *Salmonella enterica* serovar Typhimurium-derived outer membrane vesicles delivering the pneumococcal protein PspA confers protection against challenge with *Streptococcus pneumoniae*. Infect. Immun. **79:**887–894. http://dx.doi.org/10.1128/IAI.00950-10.
21. **Kim JY, Doody AM, Chen DJ, Cremona GH, Shuler ML, Putnam D, DeLisa MP.** 2008. Engineered bacterial outer membrane vesicles with enhanced functionality. J. Mol. Biol. **380:**51–66. http://dx.doi.org/10.1016/j.jmb.2008.03.076.
22. **Schroeder J, Aebischer T.** 2009. Recombinant outer membrane vesicles to augment antigen-specific live vaccine responses. Vaccine **27:**6748–6754. http://dx.doi.org/10.1016/j.vaccine.2009.08.106.
23. **Barat S, Willer Y, Rizos K, Claudi B, Maze A, Schemmer AK, Kirchhoff D, Schmidt A, Burton N, Bumann D.** 2012. Immunity to intracellular *Salmonella* depends on surface-associated antigens. PLoS Pathog. **8:**e1002966. http://dx.doi.org/10.1371/journal.ppat.1002966.
24. **Hess J, Gentschev I, Miko D, Welzel M, Ladel C, Goebel W, Kaufmann SH.** 1996. Superior efficacy of secreted over somatic antigen display in recombinant *Salmonella* vaccine induced protection against listeriosis. Proc. Natl. Acad. Sci. U. S. A. **93:**1458–1463. http://dx.doi.org/10.1073/pnas.93.4.1458.
25. **Kang HY, Curtiss R, III.** 2003. Immune responses dependent on antigen location in recombinant attenuated *Salmonella typhimurium* vaccines following oral immunization. FEMS Immunol. Med. Microbiol. **37:**99–104. http://dx.doi.org/10.1016/S0928-8244(03)00063-4.
26. **Jong WS, Soprova Z, de Punder K, ten Hagen-Jongman CM, Wagner S, Wickstrom D, de Gier JW, Andersen P, van der Wel NN, Luirink J.** 2012. A structurally informed autotransporter platform for efficient heterologous protein secretion and display. Microb. Cell Fact. **11:**85. http://dx.doi.org/10.1186/1475-2859-11-85.
27. **van Ulsen P, Rahman SU, Jong WS, Daleke-Schermerhorn MH, Luirink J.** 2014. Type V secretion: from biogenesis to biotechnology. Biochim. Biophys. Acta **1843:**1592–1611. http://dx.doi.org/10.1016/j.bbamcr.2013.11.006.
28. **Jong WS, Sauri A, Luirink J.** 2010. Extracellular production of recombinant proteins using bacterial autotransporters. Curr. Opin. Biotechnol. **21:**646–652. http://dx.doi.org/10.1016/j.copbio.2010.07.009.
29. **Jose J, Meyer TF.** 2007. The autodisplay story, from discovery to biotechnical and biomedical applications. Microbiol. Mol. Biol. Rev. **71:**600–619. http://dx.doi.org/10.1128/MMBR.00011-07.
30. **Lum M, Morona R.** 2012. IcsA autotransporter passenger promotes increased fusion protein expression on the cell surface. Microb. Cell Fact. **11:**20. http://dx.doi.org/10.1186/1475-2859-11-20.
31. **Nicolay T, Lemoine L, Lievens E, Balzarini S, Vanderleyden J, Spaepen S.** 2012. Probing the applicability of autotransporter based surface display with the EstA autotransporter of *Pseudomonas stutzeri* A15. Microb. Cell Fact. **11:**158. http://dx.doi.org/10.1186/1475-2859-11-158.
32. **Otto BR, Sijbrandi R, Luirink J, Oudega B, Heddle JG, Mizutani K, Park SY, Tame JR.** 2005. Crystal structure of hemoglobin protease, a heme binding autotransporter protein from pathogenic *Escherichia coli*. J. Biol. Chem. **280:**17339–17345. http://dx.doi.org/10.1074/jbc.M412885200.
33. **Dautin N, Barnard TJ, Anderson DE, Bernstein HD.** 2007. Cleavage of a bacterial autotransporter by an evolutionarily convergent autocatalytic mechanism. EMBO J. **26:**1942–1952. http://dx.doi.org/10.1038/sj.emboj.7601638.
34. **Jong WS, ten Hagen-Jongman CM, den Blaauwen T, Slotboom DJ, Tame JR, Wickstrom D, de Gier JW, Otto BR, Luirink J.** 2007. Limited tolerance towards folded elements during secretion of the autotransporter Hbp. Mol. Microbiol. **63:**1524–1536. http://dx.doi.org/10.1111/j.1365-2958.2007.05605.x.
35. **Roussel-Jazede V, Van Gelder P, Sijbrandi R, Rutten L, Otto BR, Luirink J, Gros P, Tommassen J, Van Ulsen P.** 2011. Channel properties of the translocator domain of the autotransporter Hbp of *Escherichia coli*. Mol. Membr. Biol. **28:**158–170. http://dx.doi.org/10.3109/09687688.2010.550328.
36. **Derouiche R, Benedetti H, Lazzaroni JC, Lazdunski C, Lloubes R.** 1995. Protein complex within *Escherichia coli* inner membrane. TolA N-terminal domain interacts with TolQ and TolR proteins. J. Biol. Chem. **270:**11078–11084.
37. **Hoiseth SK, Stocker BA.** 1981. Aromatic-dependent *Salmonella typhimurium* are non-virulent and effective as live vaccines. Nature **291:**238–239. http://dx.doi.org/10.1038/291238a0.
38. **Hashemzadeh-Bonehi L, Mehraein-Ghomi F, Mitsopoulos C, Jacob JP, Hennessey ES, Broome-Smith JK.** 1998. Importance of using *lac* rather than *ara* promoter vectors for modulating the levels of toxic gene products in *Escherichia coli*. Mol. Microbiol. **30:**676–678. http://dx.doi.org/10.1046/j.1365-2958.1998.01116.x.
39. **Datsenko KA, Wanner BL.** 2000. One-step inactivation of chromosomal genes in *Escherichia coli* K-12 using PCR products. Proc. Natl. Acad. Sci. U. S. A. **97:**6640–6645. http://dx.doi.org/10.1073/pnas.120163297.
40. **Baba T, Mori H.** 2008. The construction of systematic in-frame, single-gene knockout mutant collection in *Escherichia coli* K-12. Methods Mol. Biol. **416:**171–181. http://dx.doi.org/10.1007/978-1-59745-321-9_11.
41. **Klausen J, Magnusson M, Andersen AB, Koch C.** 1994. Characterization of purified protein derivative of tuberculin by use of monoclonal antibodies: isolation of a delayed-type hypersensitivity reactive component from *M. tuberculosis* culture filtrate. Scand. J. Immunol. **40:**345–349. http://dx.doi.org/10.1111/j.1365-3083.1994.tb03471.x.
42. **Drowart A, De Bruyn J, Huygen K, Damiani G, Godfrey HP, Stelandre M, Yernault JC, Van Vooren JP.** 1992. Isoelectrophoretic characterization of protein antigens present in mycobacterial culture filtrates and recognized by monoclonal antibodies directed against the *Mycobacterium bovis* BCG antigen 85 complex. Scand. J. Immunol. **36:**697–702. http://dx.doi.org/10.1111/j.1365-3083.1992.tb03130.x.
43. **Otto BR, van Dooren SJ, Dozois CM, Luirink J, Oudega B.** 2002. *Escherichia coli* hemoglobin protease autotransporter contributes to synergistic abscess formation and heme-dependent growth of *Bacteroides fragilis*. Infect. Immun. **70:**5–10. http://dx.doi.org/10.1128/IAI.70.1.5-10.2002.
44. **van Dooren SJ, Tame JR, Luirink J, Oudega B, Otto BR.** 2001. Purification of the autotransporter protein Hbp of *Escherichia coli*. FEMS Microbiol. Lett. **205:**147–150. http://dx.doi.org/10.1111/j.1574-6968.2001.tb10938.x.
45. **Cajo GC, Horne BE, Kelley WL, Schwager F, Georgopoulos C, Genevaux P.** 2006. The role of the DIF motif of the DnaJ (Hsp40) co-chaperone in the regulation of the DnaK (Hsp70) chaperone cycle. J. Biol. Chem. **281:**12436–12444. http://dx.doi.org/10.1074/jbc.M511192200.
46. **Chen R, Henning U.** 1996. A periplasmic protein (Skp) of *Escherichia coli* selectively binds a class of outer membrane proteins. Mol. Microbiol. **19:**1287–1294. http://dx.doi.org/10.1111/j.1365-2958.1996.tb02473.x.
47. **Baumgarten T, Vazquez J, Bastisch C, Veron W, Feuilloley MG, Nietzsche S, Wick LY, Heipieper HJ.** 2012. Alkanols and chlorophenols cause different physiological adaptive responses on the level of cell surface properties and membrane vesicle formation in *Pseudomonas putida* DOT-T1E. Appl. Microbiol. Biotechnol. **93:**837–845. http://dx.doi.org/10.1007/s00253-011-3442-9.
48. **Cox J, Mann M.** 2008. MaxQuant enables high peptide identification rates, individualized p.p.b.-range mass accuracies and proteome-wide protein quantification. Nat. Biotechnol. **26:**1367–1372. http://dx.doi.org/10.1038/nbt.1511.
49. **Pham TV, Piersma SR, Warmoes M, Jimenez CR.** 2010. On the beta-binomial model for analysis of spectral count data in label-free tandem mass spectrometry-based proteomics. Bioinformatics **26:**363–369. http://dx.doi.org/10.1093/bioinformatics/btp677.
50. **Majlessi L, Simsova M, Jarvis Z, Brodin P, Rojas MJ, Bauche C, Nouze C, Ladant D, Cole ST, Sebo P, Leclerc C.** 2006. An increase in antimycobacterial Th1-cell responses by prime-boost protocols of immunization does not enhance protection against tuberculosis. Infect. Immun. **74:**2128–2137. http://dx.doi.org/10.1128/IAI.74.4.2128-2137.2006.
51. **Schlegel S, Rujas E, Ytterberg AJ, Zubarev RA, Luirink J, de Gier JW.** 2013. Optimizing heterologous protein production in the periplasm of *E. coli* by regulating gene expression levels. Microb. Cell Fact. **12:**24. http://dx.doi.org/10.1186/1475-2859-12-24.
52. **Christiansen G, Birkelund S.** 2002. Is a chlamydia vaccine a reality? Best Pract. Res. Clin. Obstet. Gynaecol. **16:**889–900. http://dx.doi.org/10.1053/beog.2002.0324.
53. **Baehr W, Zhang YX, Joseph T, Su H, Nano FE, Everett KD, Caldwell HD.** 1988. Mapping antigenic domains expressed by *Chlamydia trachomatis* major outer membrane protein genes. Proc. Natl. Acad. Sci. U. S. A. **85:**4000–4004. http://dx.doi.org/10.1073/pnas.85.11.4000.

54. **Kim SK, DeMars R.** 2001. Epitope clusters in the major outer membrane protein of *Chlamydia trachomatis*. Curr. Opin. Immunol. **13:**429–436. http://dx.doi.org/10.1016/S0952-7915(00)00237-5.
55. **Andersen P, Andersen AB, Sorensen AL, Nagai S.** 1995. Recall of long-lived immunity to *Mycobacterium tuberculosis* infection in mice. J. Immunol. **154:**3359–3372.
56. **Kulp A, Kuehn MJ.** 2010. Biological functions and biogenesis of secreted bacterial outer membrane vesicles. Annu. Rev. Microbiol. **64:**163–184. http://dx.doi.org/10.1146/annurev.micro.091208.073413.
57. **Berlanda Scorza F, Colucci AM, Maggiore L, Sanzone S, Rossi O, Ferlenghi I, Pesce I, Caboni M, Norais N, Di Cioccio V, Saul A, Gerke C.** 2012. High yield production process for *Shigella* outer membrane particles. PLoS One **7:**e35616. http://dx.doi.org/10.1371/journal.pone.0035616.
58. **Berlanda Scorza F, Doro F, Rodriguez-Ortega MJ, Stella M, Liberatori S, Taddei AR, Serino L, Gomes Moriel D, Nesta B, Fontana MR, Spagnuolo A, Pizza M, Norais N, Grandi G.** 2008. Proteomics characterization of outer membrane vesicles from the extraintestinal pathogenic *Escherichia coli* Δ*tolR* IHE3034 mutant. Mol. Cell. Proteomics **7:**473–485. http://dx.doi.org/10.1074/mcp.M700295-MCP200.
59. **Ferrari G, Garaguso I, Adu-Bobie J, Doro F, Taddei AR, Biolchi A, Brunelli B, Giuliani MM, Pizza M, Norais N, Grandi G.** 2006. Outer membrane vesicles from group B *Neisseria meningitidis* Δ*gna33* mutant: proteomic and immunological comparison with detergent-derived outer membrane vesicles. Proteomics **6:**1856–1866. http://dx.doi.org/10.1002/pmic.200500164.
60. **Lee EY, Bang JY, Park GW, Choi DS, Kang JS, Kim HJ, Park KS, Lee JO, Kim YK, Kwon KH, Kim KP, Gho YS.** 2007. Global proteomic profiling of native outer membrane vesicles derived from *Escherichia coli*. Proteomics **7:**3143–3153. http://dx.doi.org/10.1002/pmic.200700196.
61. **Braig K, Otwinowski Z, Hegde R, Boisvert DC, Joachimiak A, Horwich AL, Sigler PB.** 1994. The crystal structure of the bacterial chaperonin GroEL at 2.8 Å. Nature **371:**578–586. http://dx.doi.org/10.1038/371578a0.
62. **Marques MA, Chitale S, Brennan PJ, Pessolani MC.** 1998. Mapping and identification of the major cell wall-associated components of *Mycobacterium leprae*. Infect. Immun. **66:**2625–2631.
63. **Boulanger A, Francez-Charlot A, Conter A, Castanie-Cornet MP, Cam K, Gutierrez C.** 2005. Multistress regulation in *Escherichia coli*: expression of *osmB* involves two independent promoters responding either to σ^S or to the RcsCDB His-Asp phosphorelay. J. Bacteriol. **187:**3282–3286. http://dx.doi.org/10.1128/JB.187.9.3282-3286.2005.
64. **Dupont M, James CE, Chevalier J, Pages JM.** 2007. An early response to environmental stress involves regulation of OmpX and OmpF, two enterobacterial outer membrane pore-forming proteins. Antimicrob. Agents Chemother. **51:**3190–3198. http://dx.doi.org/10.1128/AAC.01481-06.
65. **Aagaard C, Hoang T, Dietrich J, Cardona PJ, Izzo A, Dolganov G, Schoolnik GK, Cassidy JP, Billeskov R, Andersen P.** 2011. A multistage tuberculosis vaccine that confers efficient protection before and after exposure. Nat. Med. **17:**189–194. http://dx.doi.org/10.1038/nm.2285.
66. **Tajima N, Kawai F, Park SY, Tame JR.** 2010. A novel intein-like autoproteolytic mechanism in autotransporter proteins. J. Mol. Biol. **402:**645–656. http://dx.doi.org/10.1016/j.jmb.2010.06.068.